

Localization and conductance fluctuations in the integer quantum Hall effect: Real-space renormalization group approach

A. G. Galstyan and M. E. Raikh

Department of Physics, University of Utah, Salt Lake City, Utah 84112

Abstract

We consider the network model of the integer quantum Hall effect transition. By generalizing the real-space renormalization group procedure for the classical percolation to the case of quantum percolation, we derive a closed renormalization group (RG) equation for the universal distribution of conductance of the quantum Hall sample at the transition. We find an approximate solution of the RG equation and use it to calculate the critical exponent of the localization length and the central moments of the conductance distribution. The results obtained are compared with the results of recent numerical simulations.

PACS numbers: 73.20.Dx, 73.40.Hm, 74.20-z

I. INTRODUCTION

The fact that at zero temperature the quantum Hall transitions are infinitely narrow complicates strongly their theoretical description even without electron–electron interactions. By now, in theory, the quantitative information about the localization of two–dimensional electronic states in a magnetic field was obtained exclusively from numerical simulations. These simulations are carried out in one of two limits:

i) Short–range disorder

The results obtained before 1995 are reviewed in Refs. 1 and 2. Different approaches employed: the recursive Green’s function method³, evolution of the number of states with non–zero Chern numbers with the sample size⁴, and finite–size scaling analysis of the Thouless number^{5,6} give consistent results for the critical exponent, ν , of the localization length. Direct calculations of the conductance at the transition^{7,8} show that it is close to $0.5e^2/h$. Recent developments include the study of the role of spin–orbit scattering⁵ for spin–degenerate electrons, localization in double⁶– and multilayer systems⁹, statistics of energy levels at the transition¹⁰ and fractal properties of eigenstates at higher Landau levels¹¹.

ii) Smooth disorder

All the simulations^{12–20} were performed in the frame of the network model introduced by Chalker and Coddington¹². The questions addressed were essentially the same as in the case of the short–range disorder. In addition calculating ν ,^{12,13} the network model was used to investigate the spin–degenerate case^{14,15}, and the effect of Landau level mixing on the positions of delocalized states^{16,17}. It was also used to demonstrate that this mixing does not change the universality class of the transition¹⁸, to relate the longitudinal and transverse conductivities in the transition region¹⁹ and to trace the smearing of a single delocalized state into a metallic band in a superlattice²⁰.

Recent works^{21–28} explored the correspondence between the network model and certain limits of the models that were already studied (spin chains^{21–25}, Hubbard chains²⁶ and Dirac fermions^{27,28}).

In the recent experimental paper by Cobden and Kogan²⁹ the observation of strong and reproducible conductance fluctuations of a mesoscopic sample right at the transition was reported. This observation was also accounted for in the frame of the network model in Refs. 30 and 31. The result of simulations³¹ closely resemble the histogram of the conductance fluctuations in²⁹. In Ref. the calculated central moments of the conductance distribution were extrapolated to large sample sizes, where it becomes universal.

The network model¹² is illustrated in Fig. 1. If a disorder is smooth, classical electron drifts along equipotentials, which are closed and disconnected except for the percolation threshold. For simplicity it was assumed that at any energy equipotentials are arranged periodically. Quantum mechanics is introduced by allowing a strong tunnel coupling between the orbits when they come close enough (\sim or closer than the magnetic length). This destroys the classical localization and makes important the interference of different directed paths. Randomness is introduced by assuming the magnetic phases, acquired in course of drift along equipotentials, to be random.

If a smooth potential is symmetric with respect to zero energy, then the classical percolation threshold is also at $\varepsilon = 0$. Although this is obvious, we would like to derive the same conclusion following a different line of arguments.

The centers of closed drift trajectories in Fig. 1 form a square lattice. Classical electron switches to another trajectory, centered at a neighboring lattice site, if its energy, ε , exceeds the height, V_0 , of a saddle-point separating these sites. One can say that in this case a *bond* between two sites *connects* them. In the opposite case, $\varepsilon < V_0$, the electron retains its orbit after passing the saddle-point. Then one can say that the corresponding bond is removed. Thus we arrive at the bond percolation problem on the square lattice.

Suppose now, that the electron energy, which was initially at the lowest minimum, gradually increases. As it happens, more and more bonds switch on. Percolation occurs when some critical portion of bonds connect. It is an exact result of the percolation theory³² that for the square lattice this portion is $1/2$, which corresponds to zero energy.

The fact that the classical picture can be reformulated as a percolation problem on a

lattice suggests the following possibility. It is known that the critical exponent for classical percolation can be found with high accuracy from a simple renormalization group (RG) calculation. In course of this calculation only a small cluster is considered. If a similar approach could be devised for the quantum percolation, it would provide an approximate description of the quantum Hall transition in the closed form. In contrast to the classical renormalization scheme, such an approach should deal not with “connecting” or “removed” bonds, but characterize each bond by some scattering matrix. It should also allow for interference of different directed paths within a cluster. This program is carried out in the present paper. We utilize a real-space RG scheme for classical percolation, proposed by Reynolds, Stanley, and Klein³³, and generalize it to the quantum percolation. This generalization is described in Sec. II. We derive the RG transformation, which governs the evolution of the distribution of conductance right at the transition, with increasing the sample size. In Sec. III the approximate numerical solution for the fixed point of the RG transformation is obtained. This solution determines the universal conductance distribution at the transition. It is used for calculation of the exponent ν in Sec. IV. In this section we also discuss the finite size corrections. In Sec. V our results for the distribution of conductance of a large sample at the transition and in its vicinity are compared with recent numerical simulations. Concluding remarks are made in Sec. VI.

II. RENORMALIZATION PROCEDURE

Let us briefly remind the renormalization procedure for the classical bond percolation problem on the square lattice^{33–35}. In this procedure a fragment of original lattice containing 8 bonds (Fig. 2a) is replaced by a fragment consisting of two *superbonds*. The probability, \tilde{p} , that a superbond *does connect* two *supersites* is expressed through the corresponding probability, p , for original lattice in a following way. Firstly, the supersites are connected if all five bonds, which constitute the superbond (see Fig. 2a), connect. The probability of this is p^5 . Secondly, removing one of five bonds, does not affect the connectivity of

the superbond, the total probability of such configurations being $5p^4(1-p)$. Adding the probabilities for the superbond to connect when two and three original bonds are removed, one gets the following expression for renormalized probability.

$$\tilde{p} = p^5 + 5p^4(1-p) + 8p^3(1-p)^2 + 2p^2(1-p)^3. \quad (1)$$

The fixed point of the transformation (1), which determines the percolation threshold, is $\tilde{p} = p = 1/2$ and it coincides with the exact result. The equation for the critical exponent, ν_c , of the correlation length, ξ_c , emerges as a condition that ξ_c is the same for original and for renormalized lattices. If the lattice constant of the original lattice is a , then $\xi_c = a(\frac{1}{2} - p)^{-\nu_c}$. On the other hand, the lattice constant of the renormalized lattice is $2a$, so that $\xi_c = 2a(\frac{1}{2} - \tilde{p})^{-\nu_c}$. Assuming that $(\frac{1}{2} - p)$ and $(\frac{1}{2} - \tilde{p})$ are small, the two relations yield $\nu = \left[\ln 2 / \ln(d\tilde{p}/dp) \right]_{p=1/2}$. Using Eq. (1), one gets $\nu_c \approx 1.428$, which is only 8 percent bigger than the value $4/3$, which is presumed to be exact.

As it was mentioned in Introduction, we are interested in the situation when each bond represents a saddle-point of the random potential. Then we come to Fig. 2b, which can be viewed as a transformation of five original saddle-points into a *super-saddle-point*. In classical mechanics, p is the probability that the energy of an electron exceeds the height of the saddle-point. In quantum mechanics, a saddle-point is characterized by reflection coefficient, r , which is the amplitude for an incoming wave to retain the equipotential, or by transmission coefficient t —the amplitude to switch the equipotential. Obviously, $r^2 + t^2 = 1$. In the network, there are two incoming and two outgoing waves at each saddle-point i . The \mathbf{S} -matrix, relating the amplitudes of outgoing waves to the amplitudes of incoming waves, has the form

$$\mathbf{S}_i = \begin{pmatrix} t_i & r_i \\ r_i & -t_i \end{pmatrix}. \quad (2)$$

With five saddle-points we have five matrix equations. Solving the system, we get the following expression for the effective transmission coefficient of the super-saddle-point

$$\tilde{t} = \frac{t_1 t_5 (r_2 r_3 r_4 e^{i\Phi_2} - 1) + t_2 t_4 e^{i(\Phi_3 + \Phi_4)} (r_1 r_3 r_5 e^{-i\Phi_1} - 1) + t_3 (t_2 t_5 e^{i\Phi_3} + t_1 t_4 e^{i\Phi_4})}{(r_3 - r_2 r_4 e^{i\Phi_2})(r_3 - r_1 r_5 e^{i\Phi_1}) + (t_3 - t_4 t_5 e^{i\Phi_4})(t_3 - t_1 t_2 e^{i\Phi_3})}, \quad (3)$$

where Φ_j are the random phases acquired by an electron after traversing one of four loops shown in Fig. 2b. This expression can be viewed as a generalization of Eq. (1) to the case of quantum percolation. It appears very convenient to parametrize t_i, r_i as follows

$$t_i = \frac{1}{(e^{z_i} + 1)^{1/2}}, \quad r_i = \frac{1}{(e^{-z_i} + 1)^{1/2}}. \quad (4)$$

Then the parameter z_i can be related to the height of the saddle-point, V_i , as³⁶

$$z_i = \frac{\varepsilon - V_i}{\Gamma}, \quad \Gamma = \frac{|V_{xx}^i V_{yy}^i|^{1/2} l^2}{2\pi}. \quad (5)$$

Here ε is the energy of the electron, V_{xx}^i, V_{yy}^i are the second derivatives of the saddle-point potential, and l is the magnetic length. Thus, for $\varepsilon = 0$, z_i is the dimensionless height of the saddle-point and Eq. (3) determines the dimensionless height, $\mathbf{Z}\{z_i, \Phi_j\}$, of the super-saddle-point for a given set of z_i and Φ_j . We now introduce the distribution function

$$K(z, \{z_i\}) = \langle \delta(z - \mathbf{Z}\{z_i, \Phi_j\}) \rangle_{\{\Phi_j\}} \quad (6)$$

of the heights of super-saddle-points at given heights of original saddle-points. The averaging in (6) is carried out over the random phases Φ_j .³⁷ The crucial test for applicability of the renormalization procedure to the quantum percolation is that the position of the delocalized state should remain unchanged after renormalization. Suppose that in original lattice all z_i were zero. Then the delocalized state is at $\varepsilon = 0$. After the first step of renormalization the distribution of the heights of super-saddle-points is given by $K(z, \{z_i = 0\})$. This function is plotted in Fig. 3a. We see that it is symmetric with respect to $z = 0$, which justifies the further renormalization. Note that $z_i = 0$ at the first step, implies that the power transmission coefficient, t_i^2 , is equal to 1/2 for all saddle-points. As it follows from Fig. 3a, after the first step we already get a substantial spread in \tilde{t}^2 (the characteristic range is 0.2÷0.8). This is the result of interference of different paths, which is described by Eq. (3).

Now we can write down the renormalization group equation. Denote with $Q_n(z)$ the normalized distribution function of the heights of super-saddle-points after the n -th step of renormalization. Then the corresponding distribution function after the step $n + 1$ is given by

$$Q_{n+1}(z) = \hat{T}\{Q_n\} = \int \left(\prod_{i=1,\dots,5} dz_i \right) K(z, \{z_i\}) \prod_{i=1,\dots,5} Q_n(z_i). \quad (7)$$

The fixed point, $Q(z)$, of the transformation (7) determines the distribution of conductance of a large sample at the plateau transition. The equation for the fixed point, $Q(z) = \hat{T}\{Q\}$, is a quite complicated integral equation. In the next section we obtain its approximate solution.

III. APPROXIMATE SOLUTION OF THE RG EQUATION

The crucial observation which allows to obtain an approximate solution for the fixed-point distribution $Q(z)$ is that within the relevant region of change of the variables of integration z_i , which appears to be $\sum z_i^2 < 10$, the shape of the function $K(z, \{z_i\})$ changes rather weakly. At the same time the position of the symmetry axis of $K(z, \{z_i\})$ depends strongly on the values of z_i . In other words, the kernel of the transformation (7) can be presented as $K(z - f\{z_i\})$, where the function $K(z)$ is calculated for all $z_i = 0$ and shown in Fig. 3. By plotting $K(z, \{z_i\})$ for many sets $\{z_i\}$ (some examples are shown in Fig. 3b) we had established an approximate form of the function f :

$$f\{z_i\} = c_1(z_1 + z_2 + z_4 + z_5) + c_3 z_3 - d(z_1 - z_4)(z_2 - z_5) - \lambda_1(z_1^3 + z_2^3 + z_4^3 + z_5^3) - \lambda_3 z_3^3 + \lambda_2 z_3(z_1^2 + z_2^2 + z_4^2 + z_5^2), \quad (8)$$

with coefficients $c_1 \approx 0.416$, $c_3 \approx 0.164$, $d \approx 0.067$, $\lambda_1 \approx 0.009$, $\lambda_2 \approx 0.009$ and $\lambda_3 \approx 0.003$. The quadratic term in the expansion (8) is non-physical. It results from the deficiency of the renormalization scheme, which is the absence of complete $\pi/2$ rotational symmetry (see Fig. 2b). Fortunately, the corresponding coefficient, d , is small enough, so that this term has a small effect on $Q(z)$. We have verified it by taking this term into account as a perturbation. This term also does not affect the value of the critical exponent, ν , since it does not change upon a shift of all z_i by the same value (see below). We have also established (by first neglecting and then taking into account perturbatively) that the cubic term with

coefficient λ_2 leads to a relatively small correction to $Q(z)$. On the contrary, the cubic term with coefficient λ_1 appears to be very important.

After neglecting the quadratic and the last cubic terms in (8) the function $f\{z_i\}$ decomposes into the sum of functions of different arguments. Owing to this, a great simplification can be achieved by taking the Fourier transform of both parts in Eq. (7). One gets

$$Q_{n+1}(\omega) = K(\omega) \left[\int dz_1 Q_n(z_1) e^{i\omega(c_1 z_1 - \lambda_1 z_1^3)} \right]^4 \int dz_3 Q_n(z_3) e^{i\omega(c_3 z_3 - \lambda_3 z_3^3)}, \quad (9)$$

where $Q_n(\omega)$ is the Fourier transform of $Q_n(z)$ and $K(\omega)$ is the Fourier transform of $K(z)$. Now the solution for the fixed point $Q_n(z) = Q_{n+1}(z) = Q(z)$ can be easily obtained numerically. The result is shown in Fig. 4. Except for the tails at $|z| > 5$ it can be well approximated by a gaussian $\sqrt{\frac{\alpha}{\pi}} \exp(-\alpha z^2)$ with $\alpha \approx 0.1$. In the right-hand side of Eq. (7) there is a product of five functions $Q(z_i)$. Having $\alpha \approx 0.1$, the 5-dimensional volume, which provides the major contribution to the integral in (7), can be estimated as $\sum z_i^2 < 10$. We see that the fixed-point distribution is broad. The half-width is $z \approx \pm 2.5$, which corresponds to the range $0.08 \div 0.92$ for the power transmission coefficient. In the next section we use the solution obtained for calculation of the critical exponent ν .

IV. CRITICAL EXPONENT

We first address the critical exponent of the localization length. Suppose that before the renormalization the distribution of z is already given by $Q(z)$. Then for electron with a small but non-zero energy, ε , this distribution is given by $Q(z - z_0)$, where $z_0 = \varepsilon/\Gamma \ll 1$ (see Eq. (5)). Substituting $Q(z - z_0)$ into the right-hand side of the transformation (7) one gets a renormalized distribution, $Q(z - \tau z_0)$, where τ is some number, independent of z_0 . Upon repeating the procedure, the shift will grow as $z_0 \tau^n$ and, eventually, become ~ 1 . At this step an electron will be strongly localized in a renormalized lattice of super-saddle-points (within ~ 1 unit cell). Thus, one should identify the localization length, ξ , with a lattice constant after these n steps, which is equal to $2^n a$. Then the condition $z_0 \tau^n \sim 1$ can be rewritten as $\frac{\varepsilon}{\Gamma} \left(\frac{\xi}{a}\right)^{(\ln \tau / \ln 2)} \sim 1$, and one has $\xi \sim a \left(\frac{\varepsilon}{\Gamma}\right)^{-\nu}$ with

$$\nu = \frac{\ln 2}{\ln \tau} \quad (10)$$

The remaining task is to calculate parameter τ using Eq. (7). For small z_0 the result of substituting $Q(z - z_0)$ into the right-hand side can be presented as

$$Q(z) + z_0 \int \left(\prod_{i=1..5} dz_i \right) \left(\sum_i \frac{\partial K}{\partial z_i} \right) \prod_{i=1..5} Q(z_i) \quad (11)$$

At small z the first term behaves as $Q(0) + \frac{z^2}{2} Q_{zz}(0)$, while the second term is proportional to z (due to symmetry). As a result, the maximum of the sum (11) will get shifted from $z = 0$ to $z = z_0 \tau$, where

$$\tau = -\frac{1}{Q_{zz}(0)} \int \left(\prod_{i=1..5} dz_i \right) \left(\sum_i \frac{\partial^2 K}{\partial z \partial z_i} \Big|_{z=0} \right) \prod_{i=1..5} Q(z_i). \quad (12)$$

To proceed further we adopt the same simplification, $K(z, \{z_i\}) = K(z - f\{z_i\})$, as was adopted to find the fixed point $Q(z)$. Then one has

$$\sum_i \frac{\partial^2 K}{\partial z \partial z_i} \Big|_{z=0} = \frac{\partial^2 K}{\partial z^2}(-f\{z_i\}) \left[4c_1 + c_3 - 3\lambda_1(z_1^2 + z_2^2 + z_4^2 + z_5^2) - 3\lambda_3 z_3^2 \right]. \quad (13)$$

Note that non-physical quadratic term in (8) did not contribute to (13). After substituting (13) into (12) it is again convenient perform the Fourier transformation and then to make use of Eq. (9). Finally we get

$$\tau = 4c_1 + c_3 - 3 \frac{\int d\omega \omega^2 Q(\omega) [4\lambda_1 I_1(\omega) + \lambda_3 I_3(\omega)]}{\int d\omega \omega^2 Q(\omega)}, \quad (14)$$

where

$$I_{1,3}(\omega) = \frac{\int dz z^2 Q(z) e^{i\omega(c_{1,3}z - \lambda_{1,3}z^3)}}{\int dz Q(z) e^{i\omega(c_{1,3}z - \lambda_{1,3}z^3)}}. \quad (15)$$

Evaluating numerically the integrals in (15) and then in (14) with $Q(z)$ found in the previous section, we got for τ the value $\tau = 1.336$, which leads to the exponent $\nu = 2.39$. Since λ_1, λ_3 were determined with certain error bars, we repeated the calculations and for $\lambda_1 = 0.01$ (the effect of λ_3 is small) and got $\tau = 1.306$, $\nu = 2.59$. The results of most numerical simulations are grouped around $\nu = 2.4$.

Despite the agreement obtained, we cannot estimate the accuracy of the result, since the calculation was based on the assumption that the shape of the kernel of the transformation (7) is independent of z_i . In fact the width of the distribution $K(z, \{z_i\})$ decreases slowly with increasing $|z_i|$, and, correspondingly, $K(\omega)$ broadens. We found that at the boundary of the relevant region of the change of z_i , $\sum z_i^2 < 10$, the width of $K(\omega)$ increases by ~ 30 percent. We could not include this effect in our calculation. To obtain the limiting estimate we repeated the calculation assuming that the width of $K(\omega)$ is 30 percent bigger for *all* z_i . This caused the reduction of ν to 1.95.

In conclusion of the section let us discuss the question how the distribution $Q_n(z)$ approaches the fixed-point distribution $Q(z)$ with increasing the sample size. To answer this question let us introduce the deviation $\delta Q_n(z) = Q_n(z) - Q(z)$ and linearize the transformation (7). After using the above simplification for $K(z, \{z_i\})$ and performing the Fourier transform, we get

$$\delta Q_{n+1}(\omega) = \hat{F}\{\delta Q_n\} = K(\omega)J_1^3(\omega) \int dz \left[4J_3(\omega)e^{i\omega(c_1z - \lambda_1z^3)} + J_1(\omega)e^{i\omega(c_3z - \lambda_3z^3)} \right] \delta Q_n(z), \quad (16)$$

where

$$J_{1,3}(\omega) = \int dz Q(z) e^{i\omega(c_{1,3}z - \lambda_{1,3}z^3)}. \quad (17)$$

If initial perturbation was $\delta Q_0(z)$, then after n steps it will evolve to $\hat{F}^n\{\delta Q_0(z)\}$. The relevant perturbations are the even functions of z , satisfying the condition $\int dz Q_0(z) = 0$ (i. e. $Q_0(\omega \rightarrow 0) = 0$), to keep $Q_n(z)$ normalized. We were able to make the complete analysis of the transformation (16) only in the case $\lambda_1 = \lambda_3 = 0$. The answer is as follows. The fluctuations for which, at $\omega \rightarrow 0$, $\delta Q_0(\omega)$ behaves as ω^{2m} , m being integer, decay with increasing n as $(4c_1^{2m} + c_3^{2m})^n \propto L^{-\gamma_m}$, where $\gamma_m = \ln(4c_1^{2m} + c_3^{2m})^{-1} / \ln 2$. The slowest decay is characterized by the exponent $\gamma_1 \approx 0.5$.

With finite λ_1, λ_3 there is no such a simple classification. We could only see that the exponent increases significantly up to the value ~ 2 . At large L this exponent would

determine the finite-size correction to the conductance distribution and, thus, to the average conductance, variance and all the moments.

V. CONDUCTANCE FLUCTUATIONS

The fixed-point distribution $Q(z)$ is directly related to the distribution function of the conductance at the plateau transition. After an appropriate number of the renormalization steps the entire sample reduces to a single super-saddle-point; the power transmission coefficient of this super-saddle-point would determine the conductance of the sample, $\frac{e^2}{h}G$, with $G = (e^z + 1)^{-1}$. Then the distribution function of G can be found from the relation $P(G)dG = Q(z)dz$ yielding

$$P(G) = \frac{1}{G(1-G)}Q\left(\frac{1}{G} - 1\right). \quad (18)$$

The distribution function $P(G)$ is shown in Fig. 5. It is very broad. This fact was first pointed out in the experimental paper²⁹ and then reproduced in the numerical simulations of Cho and Fisher³¹. As a distinctive feature, the distribution function (18) has a shallow minimum at $G = 1/2$. Using this function we calculated the variance $\delta G = \sqrt{\langle G^2 \rangle - \frac{1}{4}}$ and obtained the value $\delta G = 0.33$, which agrees with the result of Ref. 31. To compare our results with the recent simulations by Wang, Jovanović and D.-H. Lee³⁰ we have calculated the moments of the distribution $P(G)$, defined as $A_n = \langle (G - \frac{1}{2})^n \rangle$, where n is an even integer which we have changed from $n = 2$ up to $n = 20$. The results are shown in Fig. 6 together with the values A_2, A_4, A_6 and A_8 , obtained in the simulations of Ref. 30. The agreement is quite good.

Finally we have studied how the variance, $\delta G(\varepsilon)$, falls off as the energy, ε , deviates from the position of the delocalized state $\varepsilon = 0$. As it was mentioned above, for non-zero energy the distribution of z is given by $Q(z - \frac{\varepsilon}{E_0})$, where $E_0 = \Gamma\left(\frac{L}{a}\right)^{-\nu}$, L being the sample size. Then one has

$$\left(\delta G(\varepsilon)\right)^2 = \int dz \frac{1}{(e^z + 1)^2} Q\left(z - \frac{\varepsilon}{E_0}\right) - \left(\int dz \frac{1}{e^z + 1} Q\left(z - \frac{\varepsilon}{E_0}\right)\right)^2. \quad (19)$$

The dependence $\delta G(\varepsilon)$ is shown in Fig. 7. To compare it with the simulations of Ref. 31 we had to establish the correspondence between our dimensionless energy ε/E_0 and the one adopted in Ref. 31. We did it by calculating the average $\langle G(\varepsilon) \rangle$ and fitting it to the curve in³¹. The agreement is again quite reasonable, especially taking into account some asymmetry of the numerical results. However, strictly speaking, the distribution of z at finite ε has the form $Q(z - \frac{\varepsilon}{E_0})$ only if ε/E_0 is smaller than 1.

Note in conclusion of the section, that identifying the conductance G with the transmission through the last super-saddle-point implies that sweeping the electron energy through $\varepsilon = 0$ causes an increase of G from 0 to 1. This was the case for the experimental geometry of Ref. 29.

VI. CONCLUSION

Certainly, the renormalization scheme for quantum percolation, developed in the present paper, provides only an approximate description of the plateau transition. As in classical percolation, when, in the course of renormalization, one ascribes a certain probability to a superbond with no care about the condition of surrounding bonds, our quantum generalization leaves out many interference processes. This happens at the stage when we average over the phases, Φ_j , in Eq. (6). By doing so we assume the phases of transmission coefficients of super-saddle-points to be uncorrelated, which in reality is not the case. However, to the best of our knowledge, the above approach is the first one in which the characteristics of the quantum Hall transition are obtained from the solution of a certain closed equation. By taking into account only basic interference processes at *each* scale, we were able to reproduce the results of numerical simulations in which *all* interference processes were taken into account. Our approach does not require extrapolation to infinite sizes. This might be important in the cases when the result of such an extrapolation is rather ambiguous. For example, when there are two (several) delocalized states *very close* in energy (Zeeman split levels, higher Landau levels). In this case the network should carry more than one chan-

nel and allow for their mixing^{14,15,18,16,17}. Formal generalization of the RG equation (7) to this case is straightforward, however its approximate solution (as in Sec. III) might be not sufficient. Note finally, that the RG results for the classical bond percolation problem can be significantly improved by considering a bigger cluster^{34,35}. Using the rules, formulated in Sec. II, this advanced scheme can be also generalized to quantum percolation.

ACKNOWLEDGMENTS

We are grateful to E. V. Tsiper for extremely valuable advises on computing.

REFERENCES

- ¹ M. Janßen, O. Viehweger, U. Fastenrath, and J. Hajdu, *Introduction to the Theory of the Integer Quantum Hall Effect*, edited by J. Hajdu (VCH, Weinheim, 1994).
- ² B. Huckestein, *Rev. Mod. Phys.*, **67**, 357 (1995).
- ³ B. Huckestein and B. Kramer, *Phys. Rev. Lett.* **64**, 1437 (1990).
- ⁴ Y. Huo and R. N. Bhatt, *Phys. Rev. Lett.* **68**, 1375 (1992).
- ⁵ C. B. Hanna, D. P. Arovas, K. Mullen, and S. M. Girvin, *Phys. Rev. B* **52** 5221 (1995).
- ⁶ E. S. Sørensen and A. H. MacDonald, *Phys. Rev. B* **54**, 10657 (1996).
- ⁷ Y. Huo, R. E. Hetzel, and R. N. Bhatt, *Phys. Rev. Lett.* **70**, 481 (1993).
- ⁸ B. M. Gammel and W. Brenig, *Phys. Rev. Lett.* **73**, 3286 (1994).
- ⁹ T. Ohtsuki, B. Kramer, and Y. Ono, *J. Phys. Soc. Jpn.*, **62**, 224 (1993).
- ¹⁰ Y. Avishai, Y. Hatsugai, and M. Kohmoto, *Phys. Rev. B* **51**, 13419, (1995).
- ¹¹ T. Terao, T. Nakayama, and H. Aoki, *Phys. Rev. B* **54**, 10350 (1996).
- ¹² J. T. Chalker and P. D. Coddington, *J. Phys. C* **21**, 2665 (1988).
- ¹³ D.-H Lee, Z. Wang, and S. Kivelson, *Phys. Rev. Lett.* **70**, 4130 (1993).
- ¹⁴ D. K. K. Lee and J. T. Chalker, *Phys. Rev. Lett.* **72**, 1510 (1994).
- ¹⁵ D. K. K. Lee, J. T. Chalker, and D. Y. K. Ko, *Phys. Rev. B* **50**, 5272 (1994).
- ¹⁶ V. Kagalovsky, B. Horovitz, and Y. Avishai, *Phys. Rev. B* **52**, R17044 (1995).
- ¹⁷ V. Kagalovsky, B. Horovitz, and Y. Avishai, preprint cond-mat/9610112 (to appear in *Phys. Rev. B*, March 1997).
- ¹⁸ Z. Wang, D.-H. Lee, and X.-G. Wen, *Phys. Rev. Lett.* **72**, 2454 (1994).

- ¹⁹ I. Ruzin and S. Feng, Phys. Rev. Lett. **74**, 154 (1995).
- ²⁰ J. T. Chalker and A. Dohmen, Phys. Rev. Lett. **75**, 4496 (1995).
- ²¹ D.-H. Lee, Phys. Rev. B **50**, 10788 (1994).
- ²² M. R. Zirnbauer, Ann. Phys. (Leipzig) **3**, 513 (1994).
- ²³ Y. B. Kim, Phys. Rev. B **53**, 16420 (1996).
- ²⁴ J. Kondev and J. B. Marston, preprint, cond-mat/9612223.
- ²⁵ I. A. Gruzberg, N. Read, and S. Sachdev, preprint cond-mat/9612038 (1996).
- ²⁶ D.-H. Lee and Z. Wang, Phil. Mag. **73**, 145 (1996).
- ²⁷ A. W. W. Ludwig, M. P. A. Fisher, R. Shankar, and G. Grinstein, Phys. Rev. B **50**, 7526 (1994).
- ²⁸ C.-M. Ho and J. T. Chalker, Phys. Rev. B **54**, 8708 (1996).
- ²⁹ D. H. Cobden and E. Kogan, Phys. Rev. B **54**, R17316 (1996).
- ³⁰ Z. Wang, B. Jovanović, and D.-H. Lee, Phys. Rev. Lett. **77**, 4426 (1996).
- ³¹ S. Cho and M. P. A. Fisher, preprint cond-mat/9609048, (to appear in Phys. Rev. B, January 1997).
- ³² D. Stauffer and A. Aharony, *Introduction to Percolation Theory* (Taylor and Francis, London, 1992).
- ³³ P. J. Reynolds, H. E. Stanley, and W. Klein, J. Phys. C, **10**, L167 (1977).
- ³⁴ P. J. Reynolds, H. E. Stanley, and W. Klein, Phys. Rev. B **21**, 1223 (1980).
- ³⁵ J. Bernasconi, Phys. Rev. B **18**, 2185 (1978).
- ³⁶ H. A. Fertig and B. I. Halperin, Phys. Rev. B **36**, 7967 (1987).

³⁷ Similar procedure was previously used by T. V. Shahbazyan and one of the authors, Phys. Rev. Lett. **75**, 304 (1995).

FIGURES

FIG. 1. Schematic representation of the network model. Circles show equipotentials. Dashed lines show the saddle-points.

FIG. 2. Schematic illustration of the renormalization procedure for the classical (a) and quantum (b) percolation.

FIG. 3. Distribution of heights of the super-saddle-points $K(z, \{z_i\})$ is plotted for different sets $\{z_1, z_2, z_3, z_4, z_5\}$; (a) $\{0,0,0,0,0\}$; (b) $\{-2,2,0,-1,1\}$ (solid curve), $\{-1.5,-1.5,-2,-1.5,-1.5\}$ (dotted curve), $\{-1.5,1.5,0,-1.5,-1.5\}$ (dashed-dotted curve), $\{1,-1,2,1,5,0.5\}$ (short-dashed curve) $\{1,2,2,1,2\}$ (long-dashed curve).

FIG. 4. Fixed-point distribution of heights of the super-saddle-points.

FIG. 5. Distribution function of conductance at the quantum Hall transition.

FIG. 6. Moments $A_n = \langle (G - \frac{1}{2})^n \rangle$ of the conductance distribution at the transition are shown for different n . Diamonds show the numerical results of Ref. 30.

FIG. 7. Variance of the conductance fluctuations is plotted v.s. dimensionless energy.

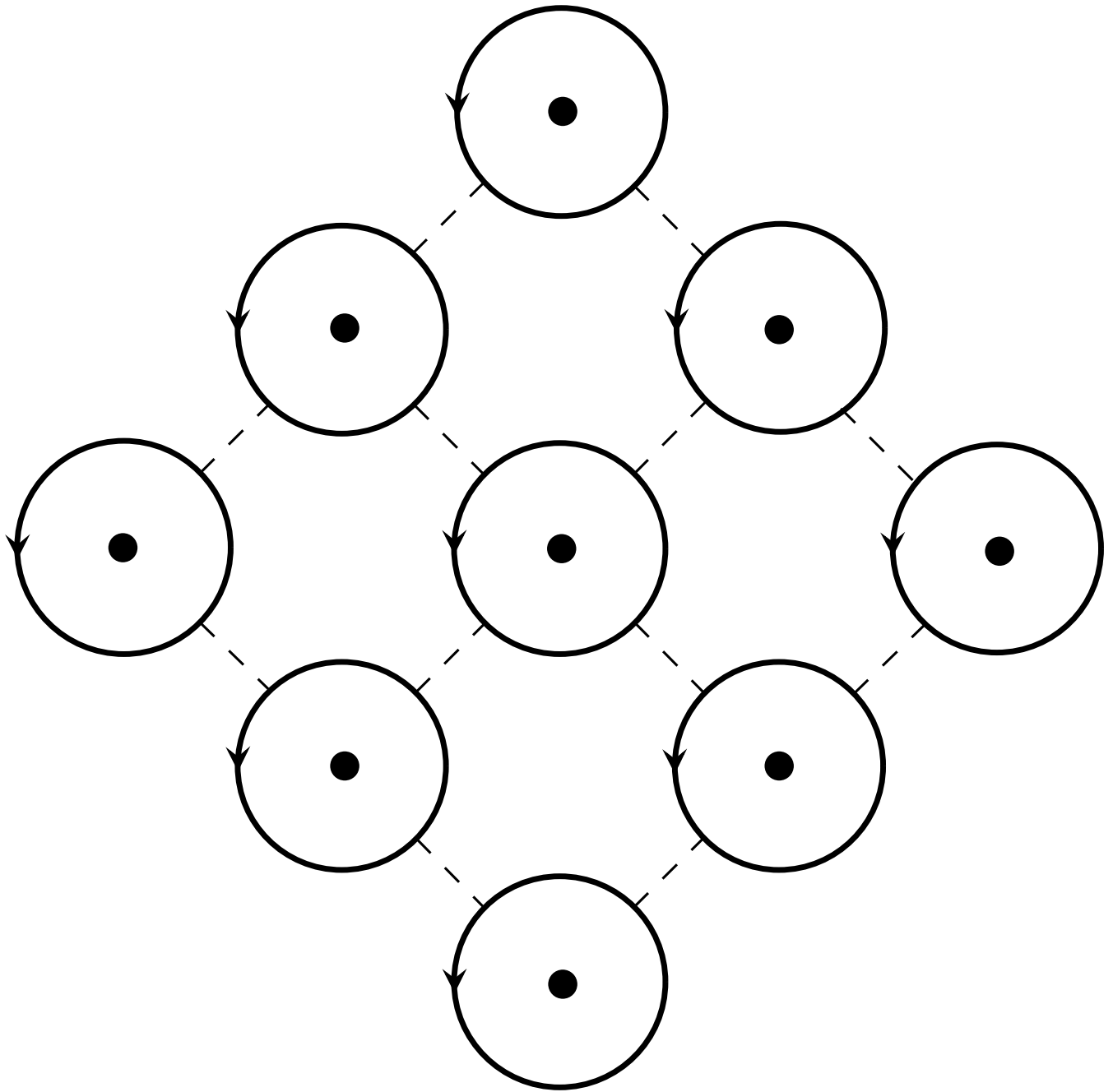
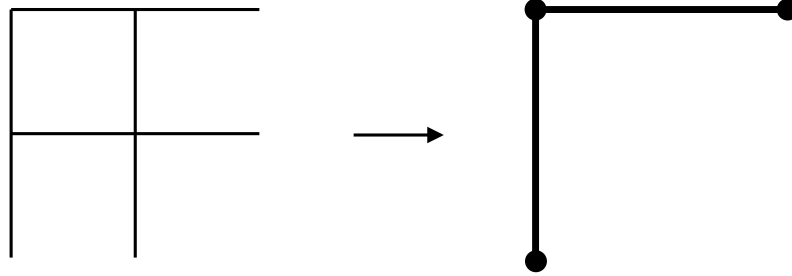


Fig. 1

a)



b)

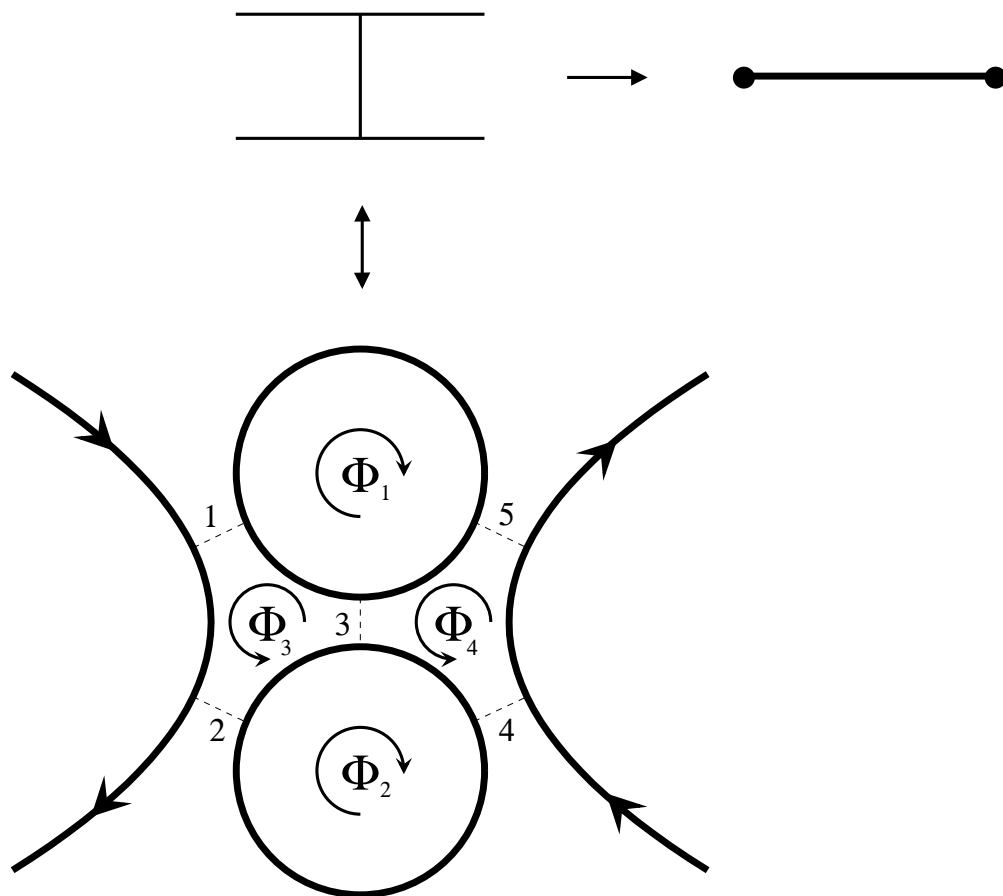
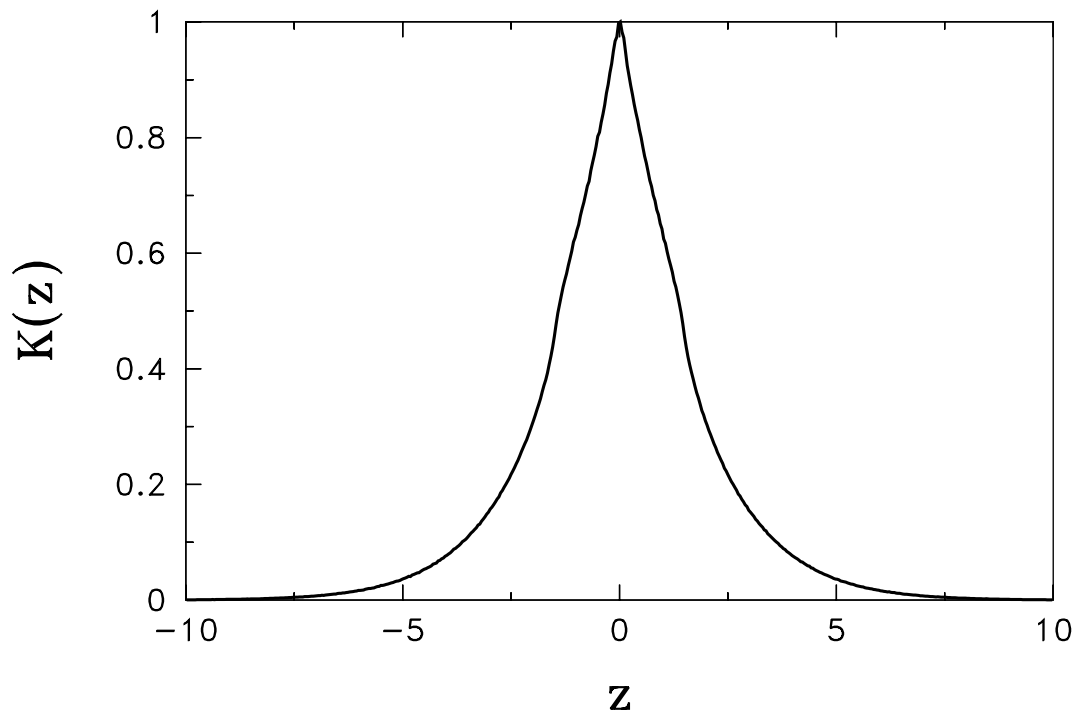


Fig. 2

a)



b)

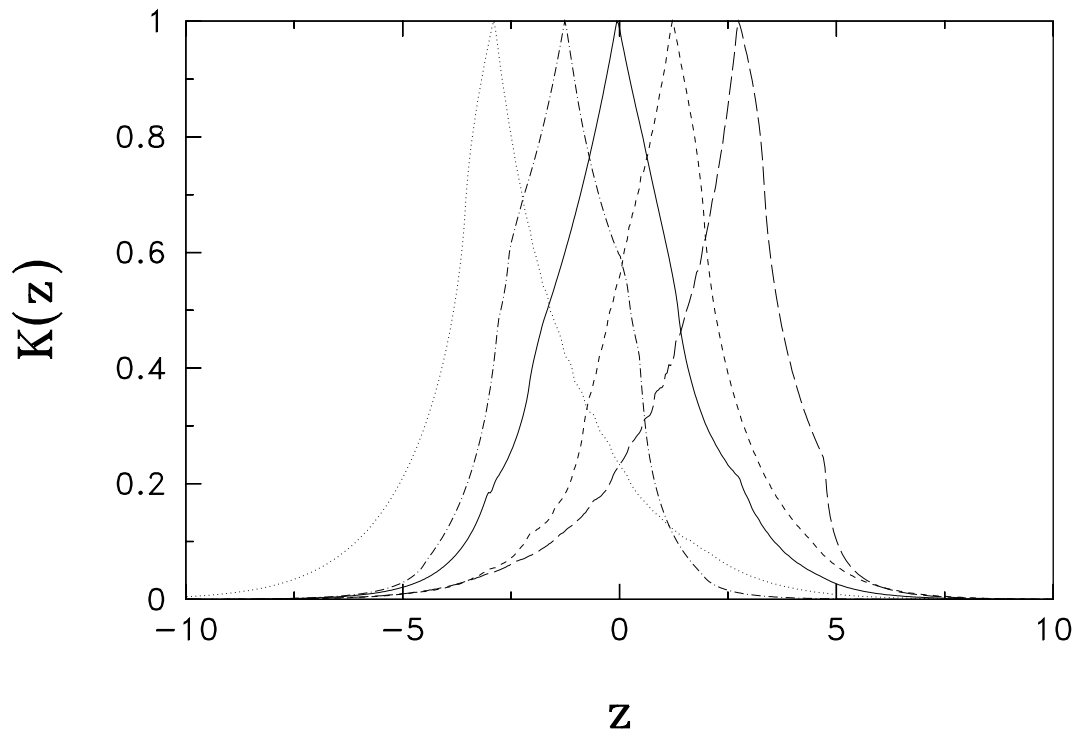


Fig. 3

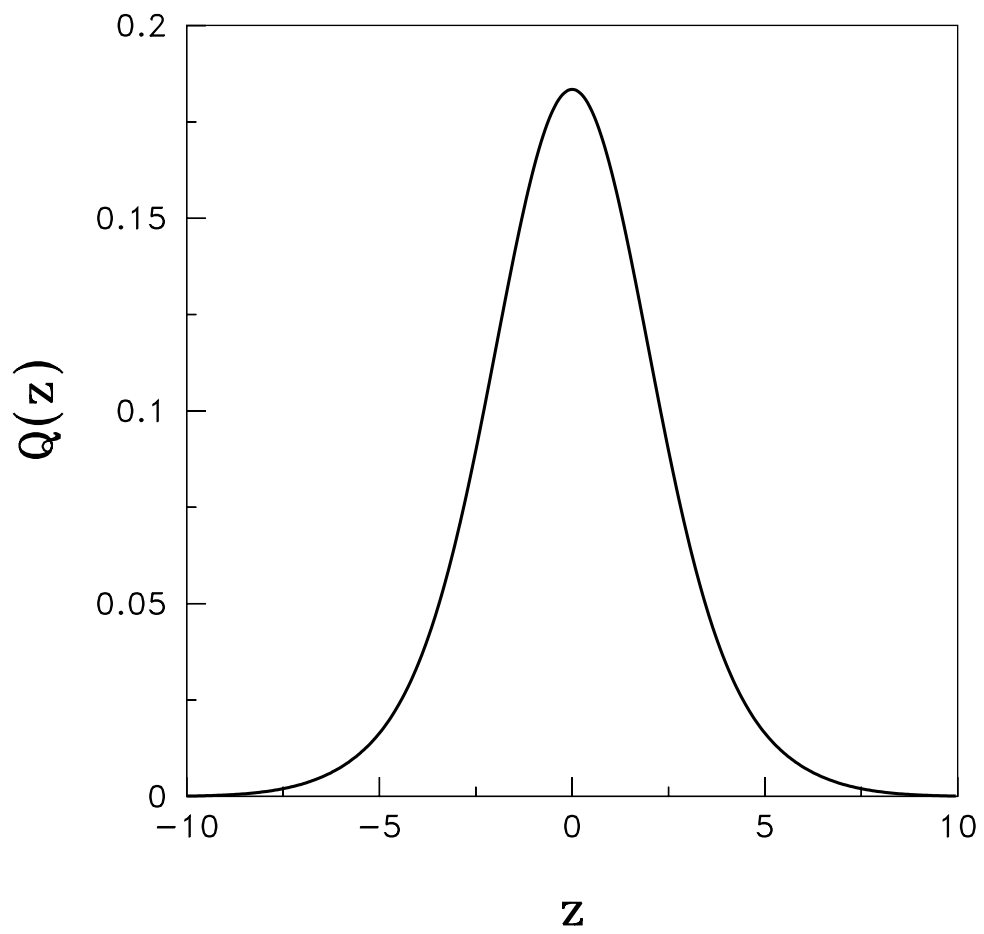


Fig. 4

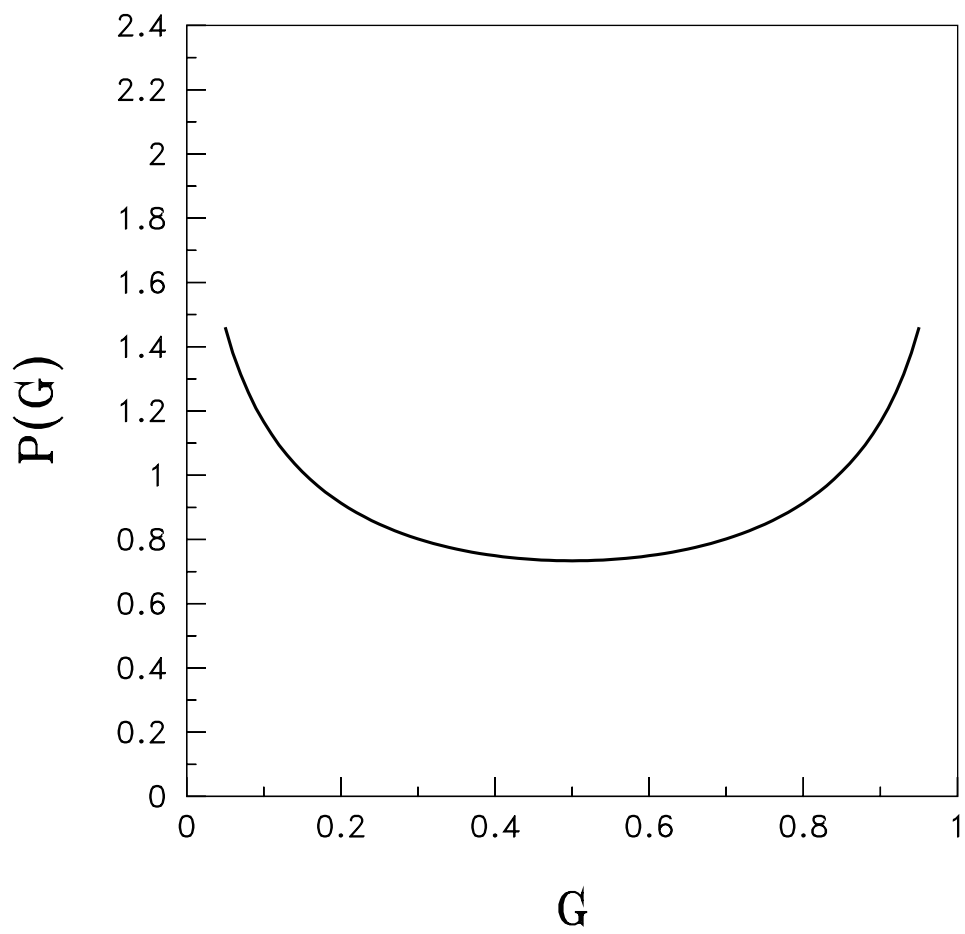


Fig. 5

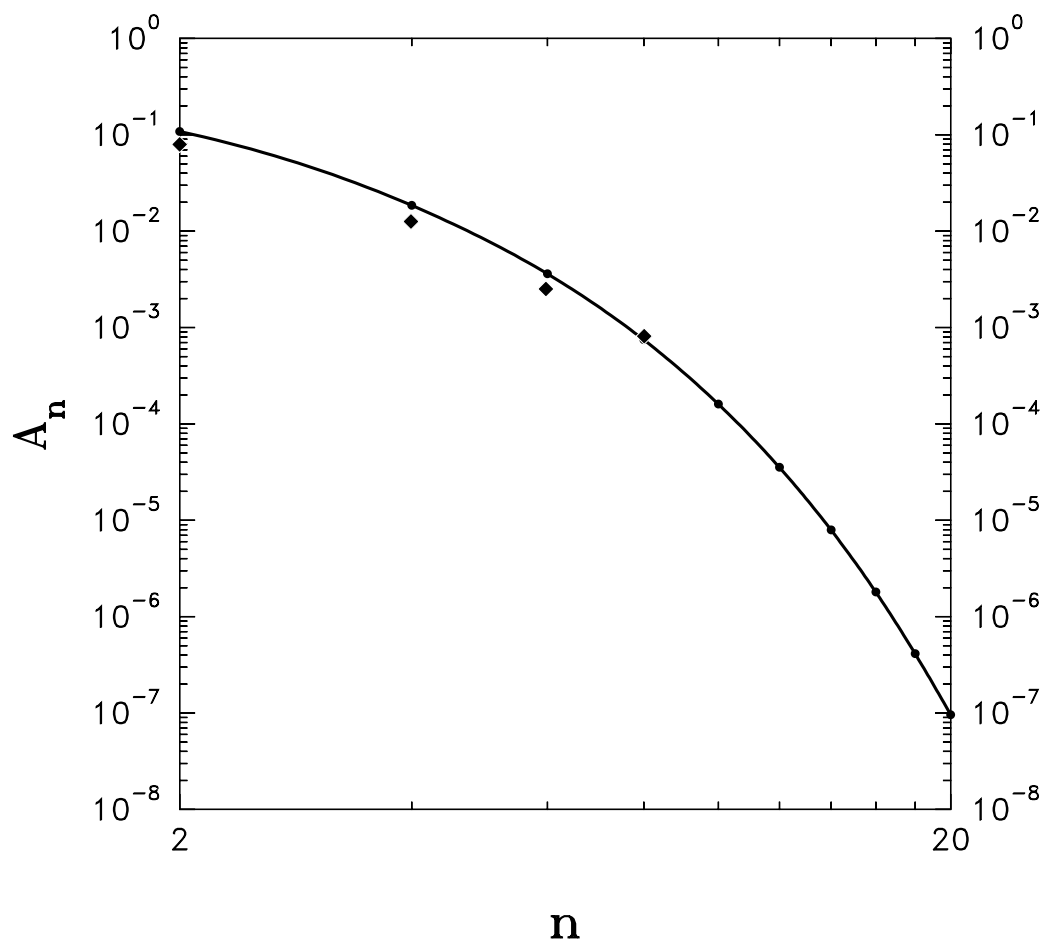


Fig. 6

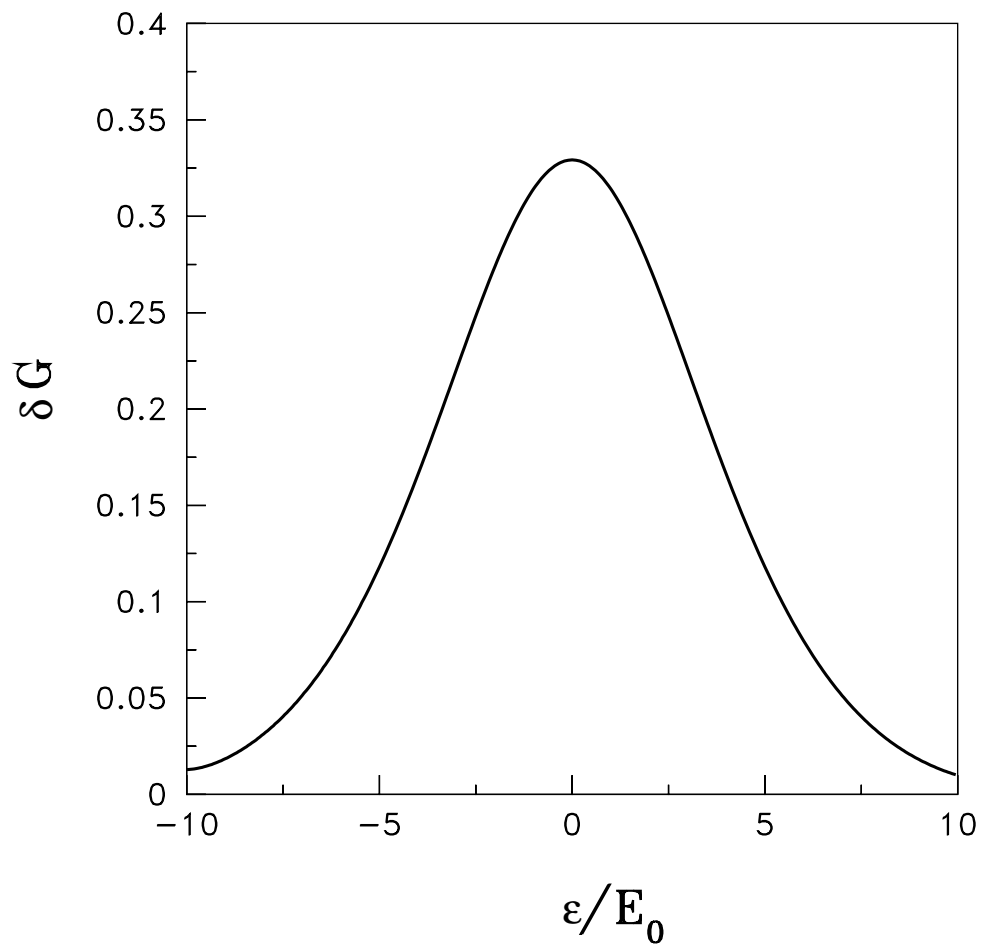


Fig. 7